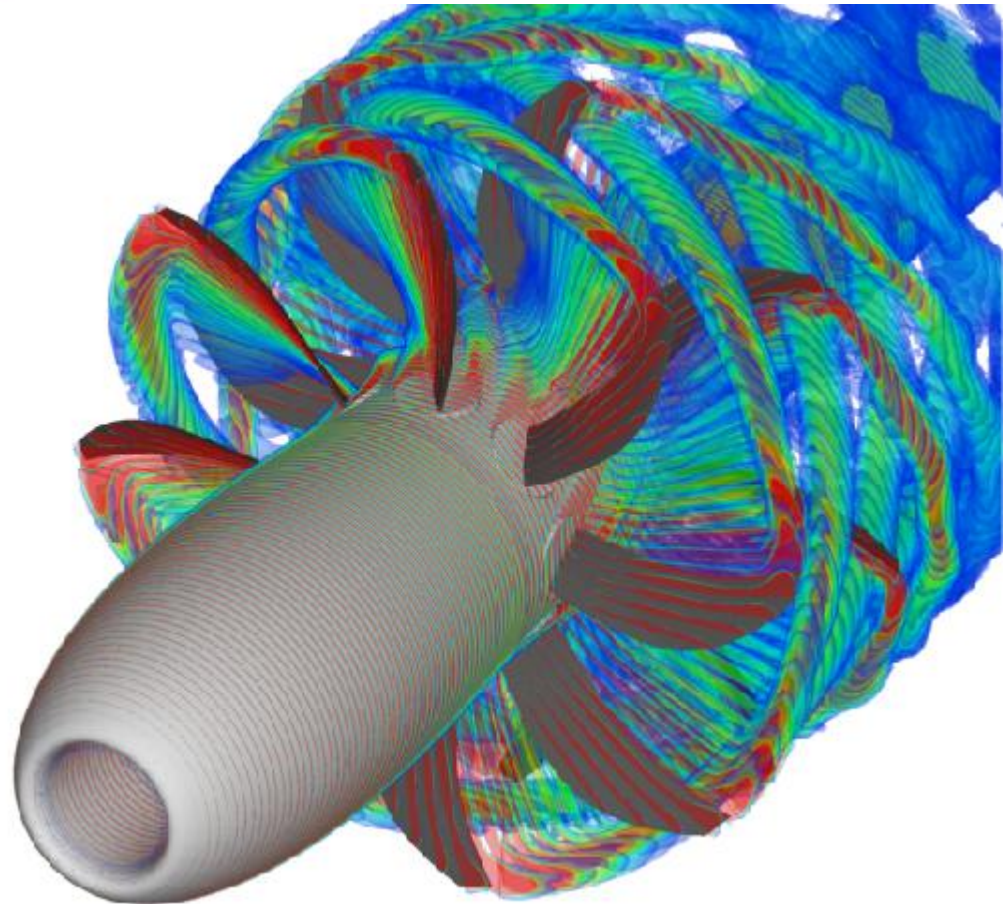


Numerical Analysis of CROR Propulsion System Aerodynamics & Aeroacoustics at DLR

Arne Stuermer &
Jianping Yin
Institute of Aerodynamics &
Flow Technology
DLR Braunschweig
Germany

2nd UTIAS-MITACS
International Workshop on
Aviation & Climate Change
May 27th-28th, 2010
UTIAS
Toronto, Canada



Overview

- Introduction and Motivation
- DLR-AS CROR Activities Overview
- Generic Research Geometry and Test Case Definition
- Aerodynamics & Aeroacoustics @ Low-Speed and High-Speed:
 - Numerical Tools and Approaches
 - Flow Physics Analysis and Comparison
- Conclusion and Outlook

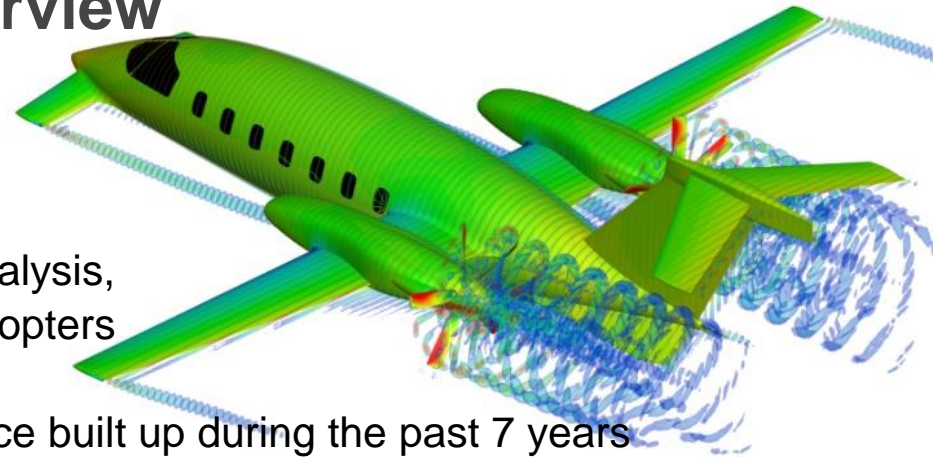


Introduction and Motivation



- Cost of fuel has led to a renaissance of the Contra-Rotating Open Rotor (CROR)
- Propfans studied in NASA/US Industry Advanced Turboprop Project (ATP)
 - Comprehensive research on aerodynamics and aeroacoustics, demonstrating significant efficiency benefits
 - Flight tests of prototype engines on McDonnell Douglas MD-80 and Boeing 727
 - Close to EIS in 1990s on proposed McDonnell Douglas MD-90XX & Boeing 7J7
 - Drop in fuel prices lead to waning of interest for airlines
- Concern about high fuel costs are back ('08: 33% of TOC; '98:9.4% of TOC)
- Installation, noise and certification issues still remain:
 - Modern methods could play vital role in realizing full potential of CRORs for EIS ~2020

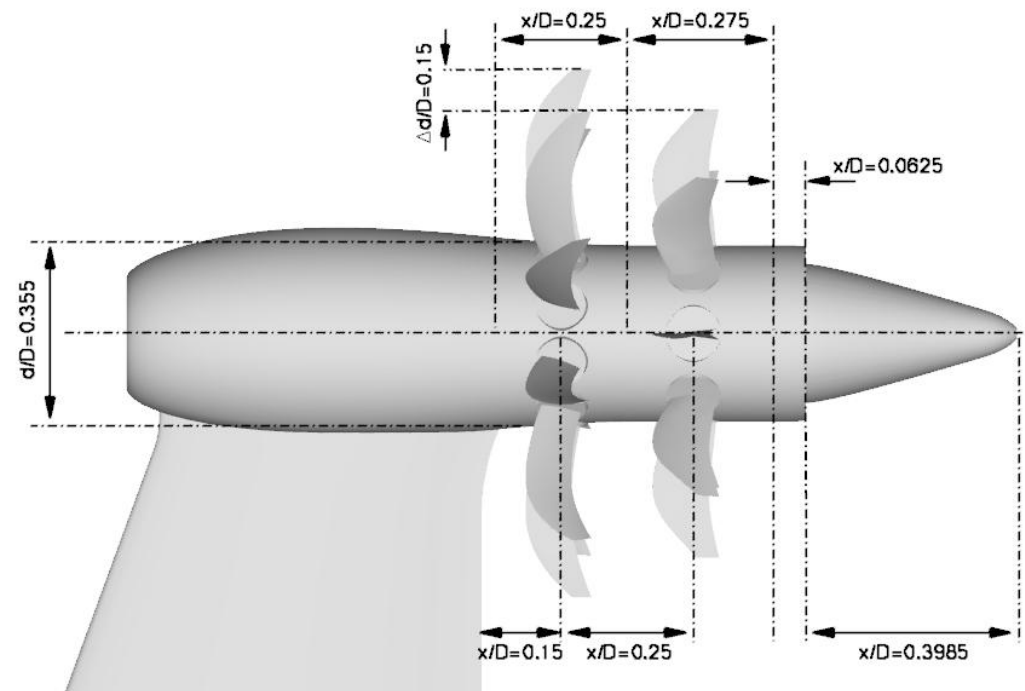
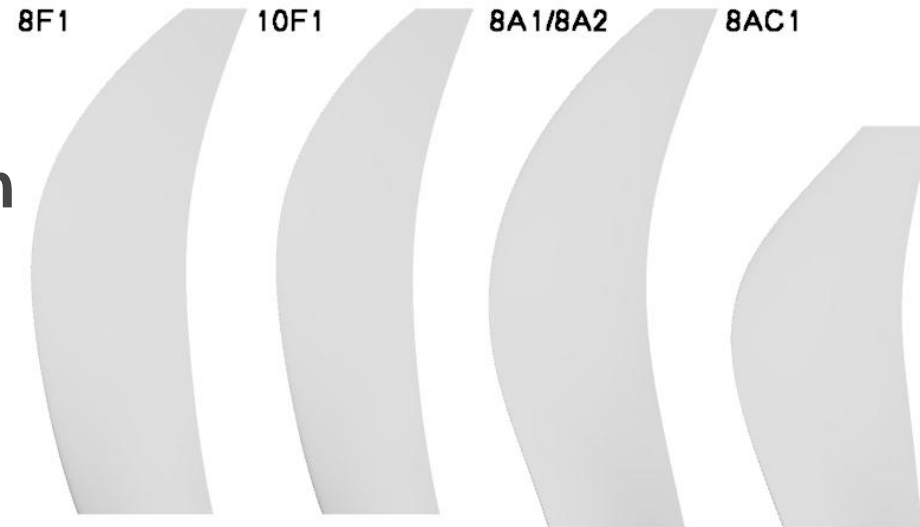
DLR CROR Activities Overview



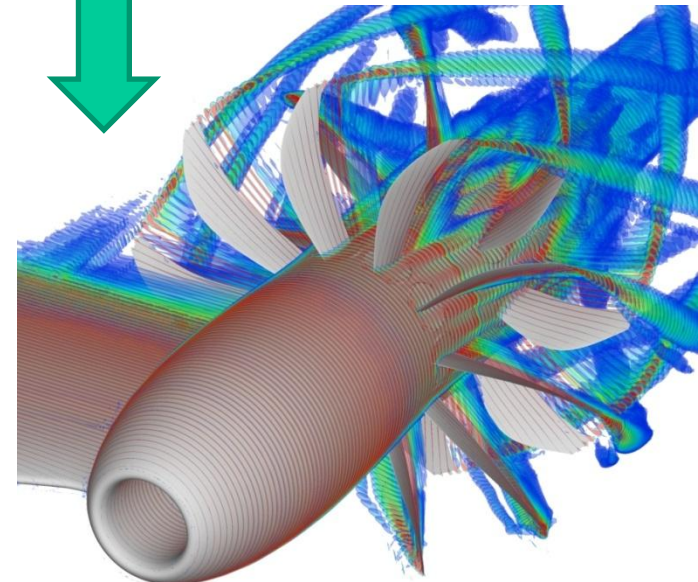
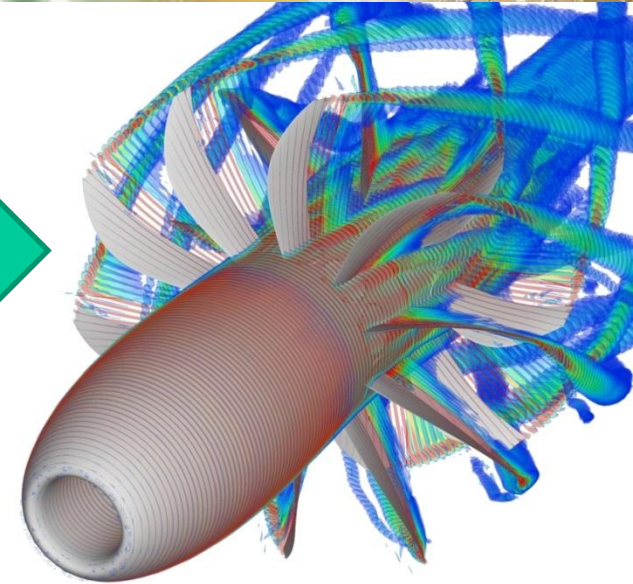
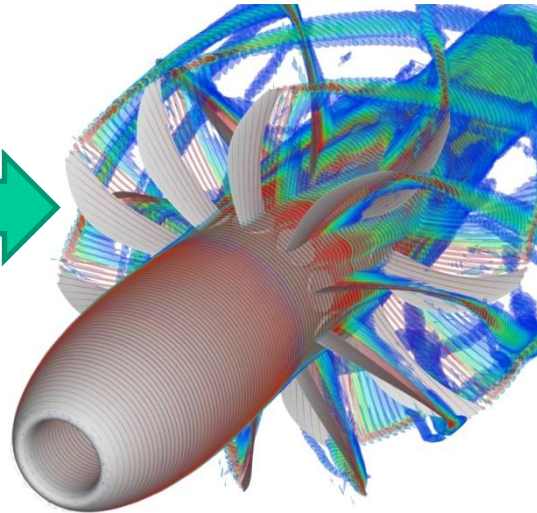
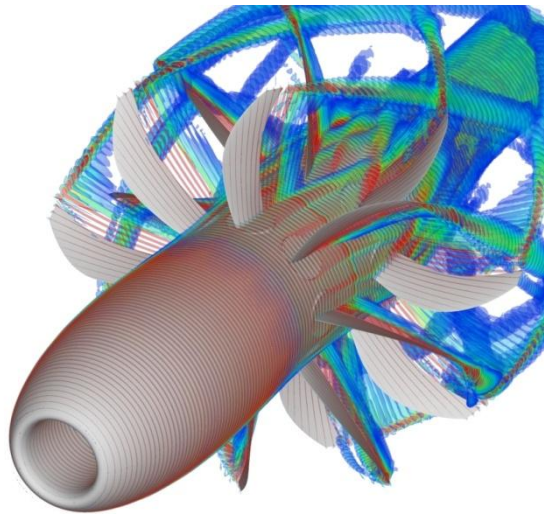
- History of experimental & numerical analysis, design & testing of propellers and helicopters
- DLR-AS CFD-based analysis experience built up during the past 7 years
 - Coupled CFD-CAA (TAU/APSIM) analysis process chain established
 - Cooperation with Industry on SRP-related topics
 - EU FP6 project CESAR (Cost Effective Small AiRcraft)
 - CROR activities since 2007
 - Generic studies based on in-house designed research configurations
 - Cooperation with & contract work for airframe and propulsion industrial partners
 - DLR-AT/AS involvement in EU FP7 project DREAM (validation of Radical Engine Architecture systems)
 - Associated Partner in CROR activities in JTI SFWA WP2.2
 - Partnership with industry in nationally funded projects

Research Geometry: Sizing, Nacelle and Pylon

- Generic CROR to test and mature numerical methods and approaches and improve understanding
- Sized for 150-seat aircraft:
 - TO-thrust ~88kN
 - Cruise thrust ~19kN
- D=14ft/4.2672m propeller
- Family of blade designs
 - 8- & 10-blade front rotor
 - 14ft & 11.9ft 8-blade aft rotor
 - Generic pylon
- CATIA V5-CAD model and mesh generation setup for flexibility in terms of configuration variations



Systematic Configuration Studies



- Investigation of configuration impact on performance and noise
- Blade number variation: 8x8 to 10x8
- Aft rotor diameter reduction to eliminate tip vortex impingement
- Addition of pylon to investigate installation effect impact
- Representative performance levels:

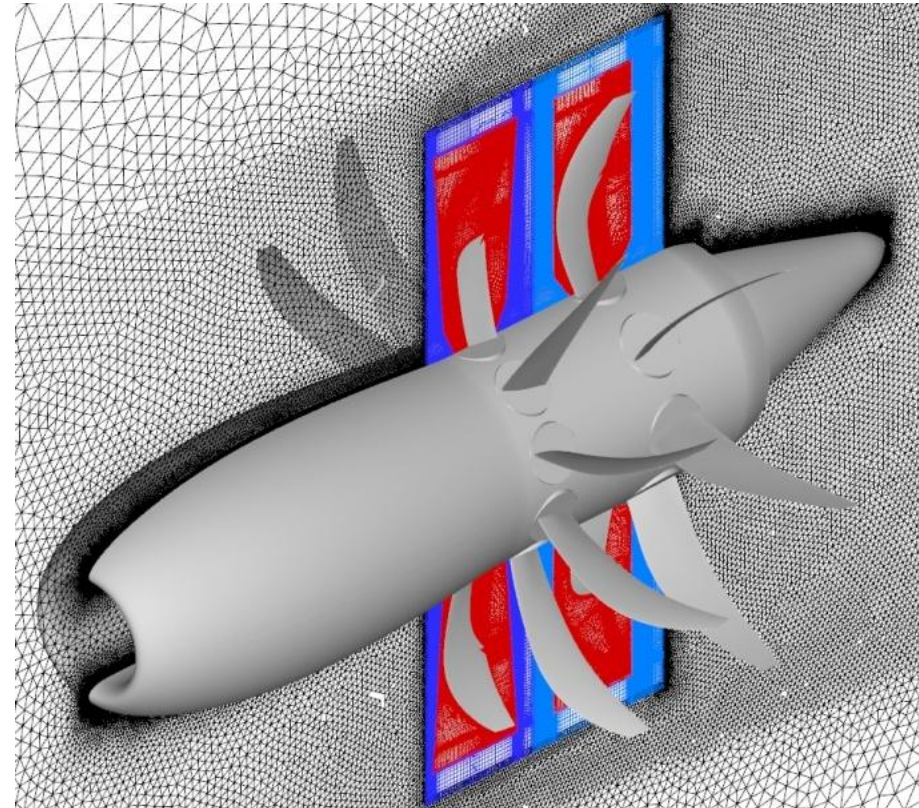
Cruise Performance of 10F2x8AC1 CROR
M=0.75 @ h=35,000ft; J₁=3.678, J₂=4.203

| | Rotor 1 | Rotor 2 | Total |
|--------------------------|----------------|----------------|--------------|
| F_x [N] | 10,566 | 8,424 | 18,990 |
| η [%] | 79.72 | 91.98 | 85.85 |



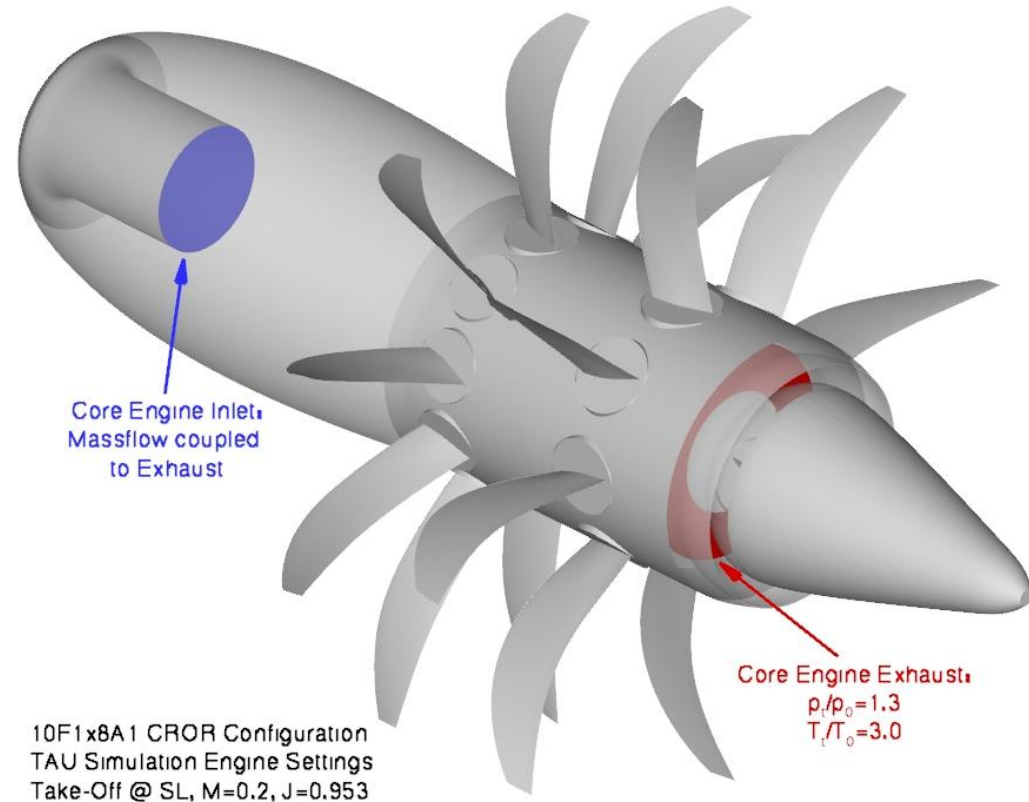
Numerical Approach: Geometry & Mesh Generation

- Unstructured/structured mesh generation with CentaurSoft Centaur and ICEM CFD HEXA
- 19-21 mesh blocks used to fully exploit flexibility of Chimera approach
- Hub PCM geometry introduced to allow flexible adjustment of blade pitch angles
- Special care taken @ Chimera boundaries and for viscous sublayer resolution
- Rotor Chimera boundary can serve as interface to aeroacoustic tools
- Total mesh sizes ~45, 000,000 nodes



Test Case Definition: Low-Speed Cases

- Take-Off @ SL and $M=0.2$, $\alpha=0^\circ$
- Identical propeller rotational speeds
- TAU engine boundary condition to simulate realistic inlet and jet flows
- Blade settings for a 50:50 power split



| | Core engine exhaust | | $n_1=n_2$ [rpm] | $J_1=J_2$ | $\beta_{75,R1}$ [°] | $\beta_{75,R2}$ [°] |
|-----------------|---------------------|-----------|-----------------|-----------|---------------------|---------------------|
| | ρ_t/ρ_0 | T_t/T_0 | | | | |
| 8F1x8A1 | 1.3 | 3.0 | 1029 | 0.953 | 37.6 | 36.25 |
| 10F1x8A1 | 1.3 | 3.0 | 1029 | 0.953 | 36.5 | 36.15 |

The DLR TAU-Code

Code Description and Simulation Approach

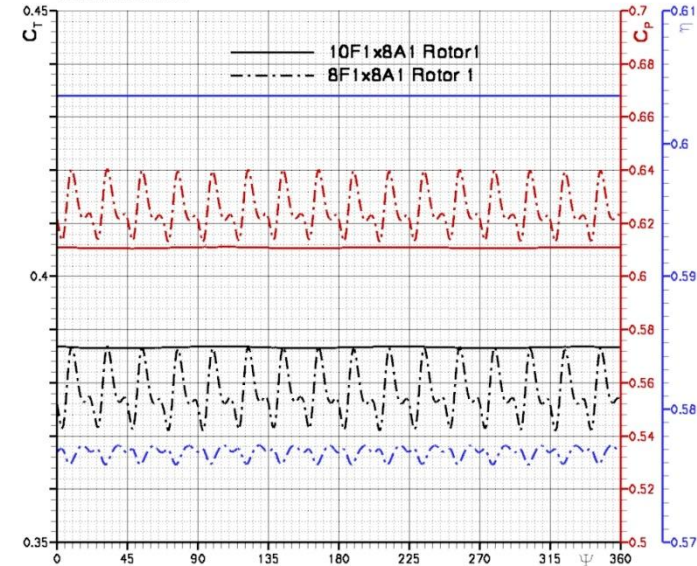
- Unstructured finite volume Euler/RANS-flow solver
- All standard state-of-the-art CFD techniques available:
 - Central and upwind schemes for spatial discretization
 - Scalar or Matrix dissipation
 - Multistage Runge-Kutta time-stepping, LUSGS
 - Convergence acceleration through MG, residual smoothing, local time-steps
 - 1- and 2-equation turbulence models (SAE, k- ω SST)
- Chimera grid approach & extensive motion libraries for rotating propeller computations
- Dual time stepping scheme for unsteady computations
- Efficiently parallelized for fast-turn around times through distributed computing
- Typically ~6 rotor revolutions computed on 256-384 CPUs of DLR C²A²S²E-cluster
- Runtime ~ 14-21 days wallclock

Rotor Performance

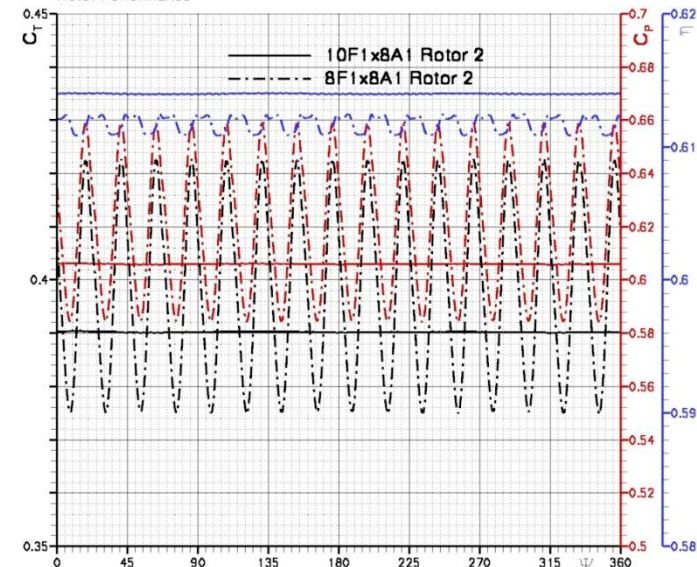
| | 8F1x8A1 | | | 10F1x8A1 | | |
|------------|---------|---------|--------|----------|---------|--------|
| | Rotor 1 | Rotor 2 | Total | Rotor 1 | Rotor 2 | Total |
| F_x [N] | 42,994 | 45,233 | 88,226 | 43,952 | 44,357 | 88,309 |
| C_T | 0.3782 | 0.3979 | - | 0.3867 | 0.3902 | - |
| C_P | 0.6253 | 0.6203 | - | 0.6108 | 0.6059 | - |
| η [%] | 57.67 | 61.17 | 59.42 | 60.36 | 61.39 | 60.88 |

- 8x8 CROR shows 16/32 cycle oscillations in rotor loads
- $F_x=88.226$ kN; $C_{T,1}/C_{T,2}=0.9523$; $C_{P,1}/C_{P,2}=1.0042$
- Larger amplitudes in aft rotor
- 50:50 power split leads to higher aft rotor thrust
- Better efficiency in aft rotor
- 10x8 configuration has constant rotor loads
- $F_x=88.309$ kN; $C_{T,1}/C_{T,2}=0.9909$; $C_{P,1}/C_{P,2}=1.0017$
- 10x8 more thrust for rotor 1, less for rotor 2 than 8x8
- 10x8 less power for rotor 1 and rotor 2

10F1x8A1 vs 8F1x8A1 for TO @ SL, M=0.2, $\alpha=0^\circ$
Rotor Performance



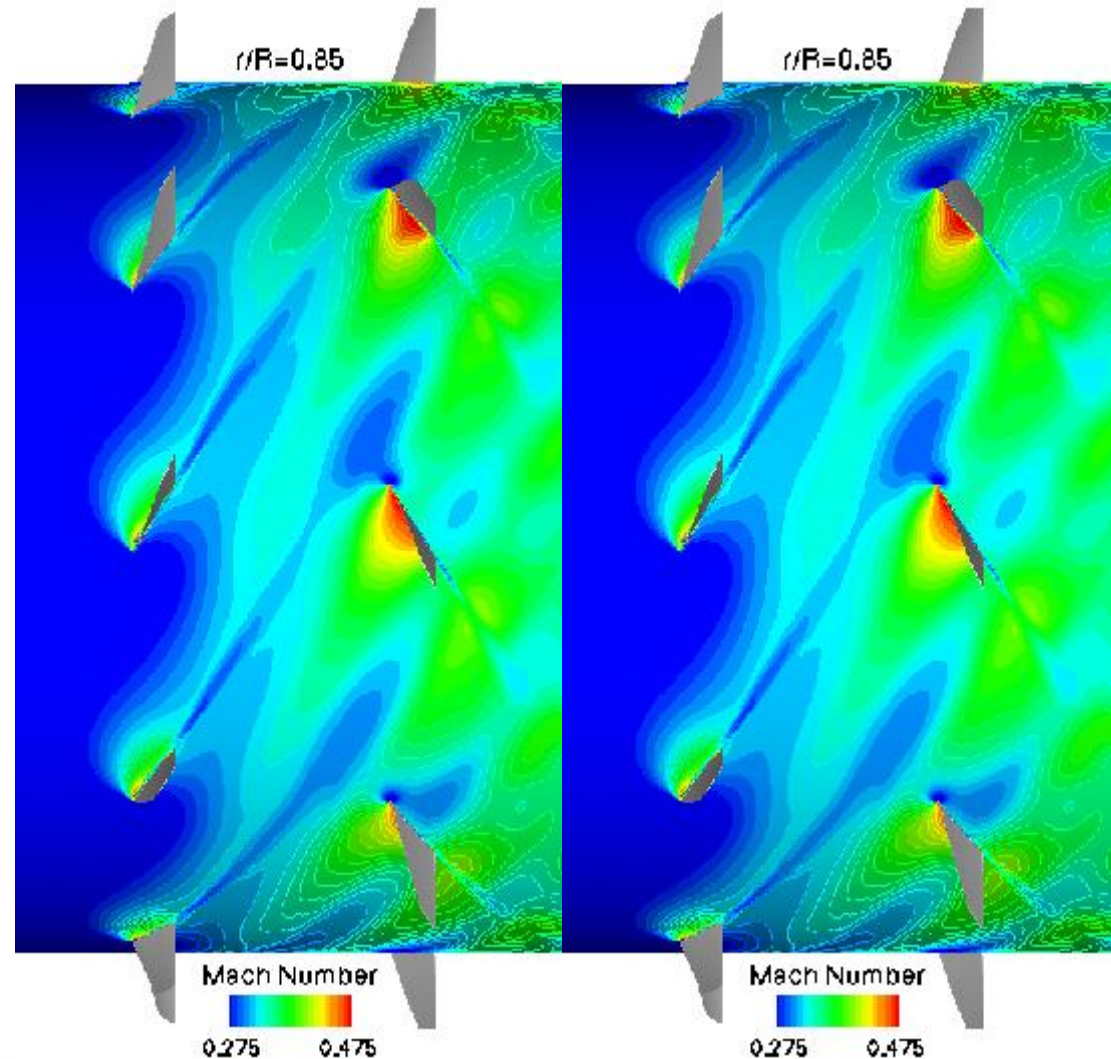
10F1x8A1 vs 8F1x8A1 for TO @ SL, M=0.2, $\alpha=0^\circ$
Rotor Performance



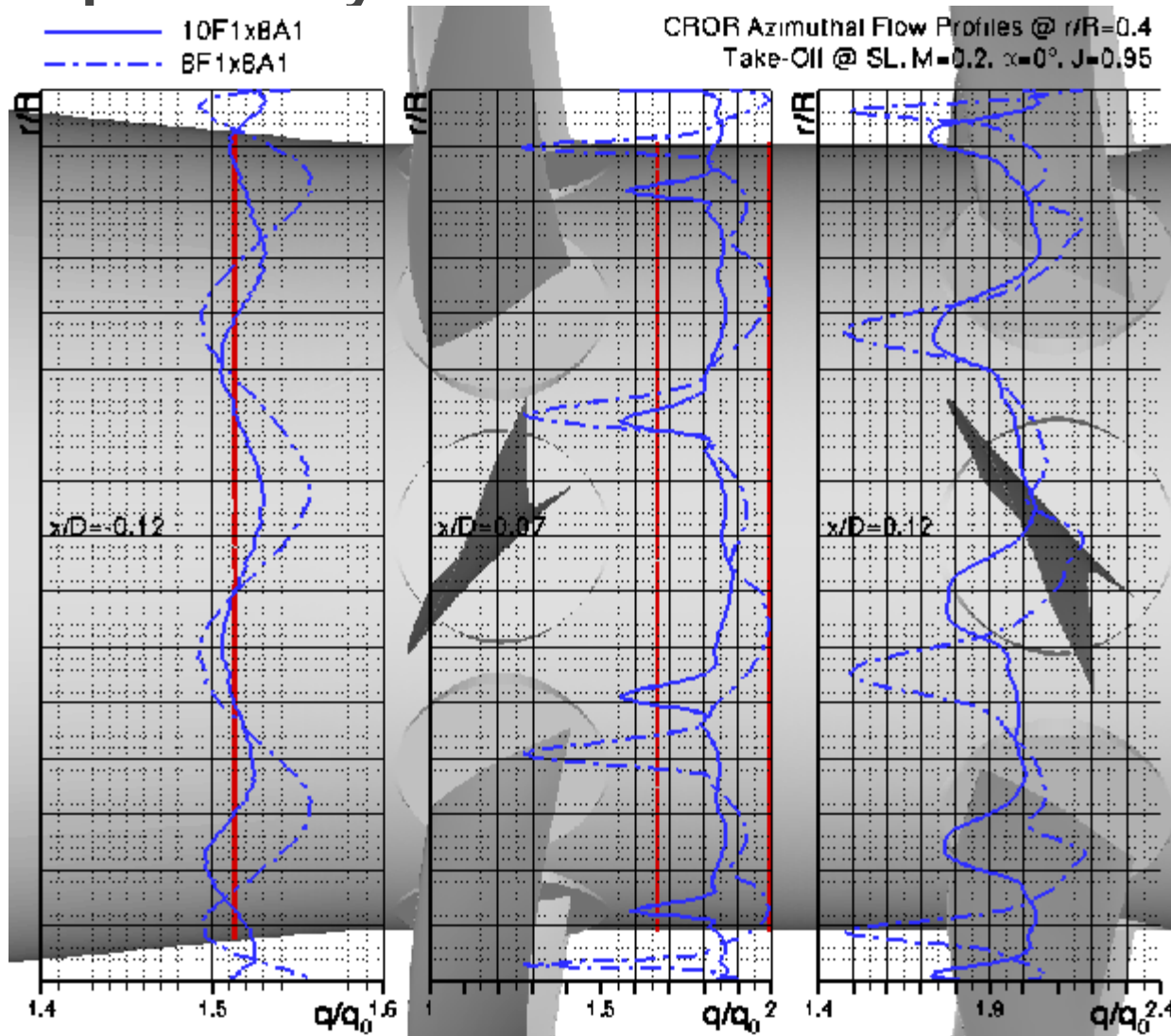
Slipstream Development: Blade Wakes @ $r/R=0.85$

10x8 CROR

- Strong blade wakes, quite well resolved in simulations
- Good functionality of Chimera boundary condition, with smooth transition of contour lines (blade-rotor, rotor-rotor, rotor-nacelle)
- Mutual interactions between rotors:
 - Aft blades influenced by forward rotor blade wakes
 - Aft blade wakes interact with “sliced” forward blades wakes
 - 16-cycle oscillations seen on forward blades pressure side Mach number distributions
 - Small Mach number fluctuations upstream of front rotor



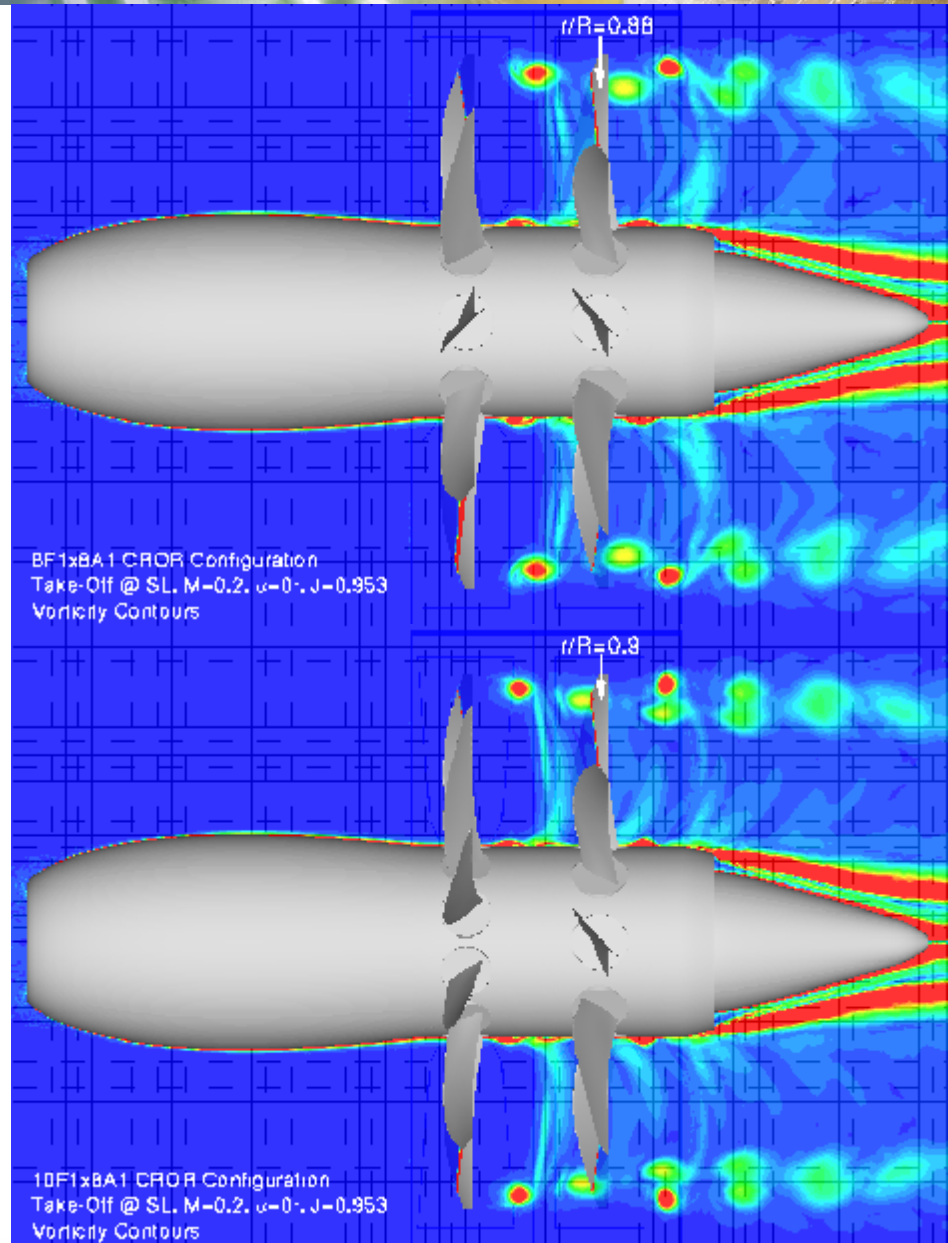
Slipstream Development: Dynamic Pressure Profiles



- 3 axial wake profiles at $r/R=0.4$
- Dynamic pressure increases after first and second rotor
- R1 Blade wakes:
 - Stronger for 8x8 CROR
- R1 potential flow:
 - Stronger for 8x8 CROR
- R2 potential flow seen in fluctuation of wake profiles
- Two important sources of interaction tone generations

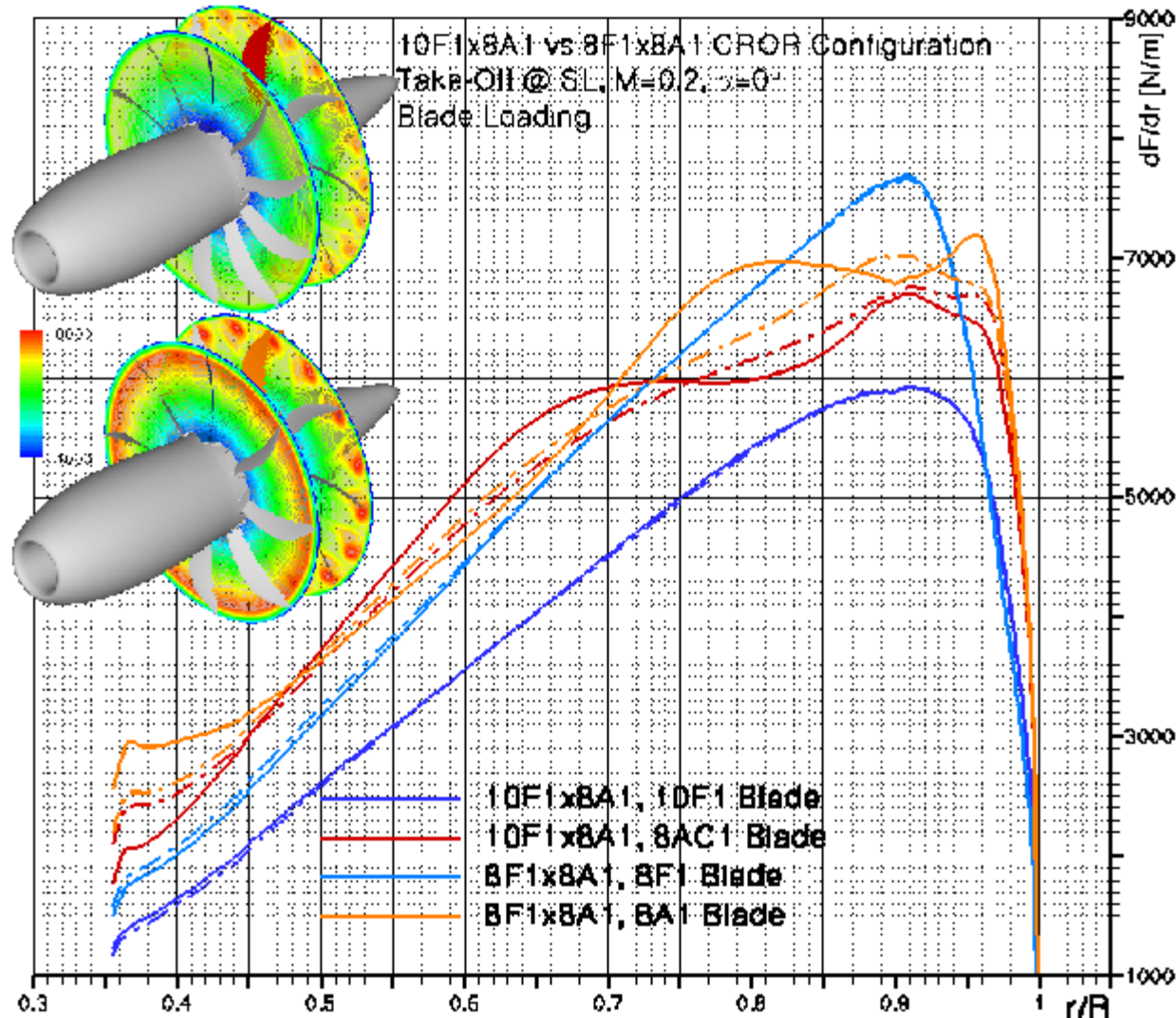
Slipstream Development: Tip Vortex Trajectory

- Investigation of front rotor tip vortex impact on aft rotor blades on noise emissions
- Comparison of vortex track for 10F1x8A1 & 8F1x8A1 CROR:
 - Stronger front rotor slipstream contraction for the 8x8 CROR due to higher blade loadings
 - Vortex impact on aft rotor occurs @ $r/R=0.9$ for 10x8 and $r/R=0.88$ for 8x8
- Guide for blade design of reduced diameter aft rotor
 - 8AC1-blade has a 15%-crop in diameter



Blade Load Distributions: 8F1x8A1 vs 10F1x8A1 CROR

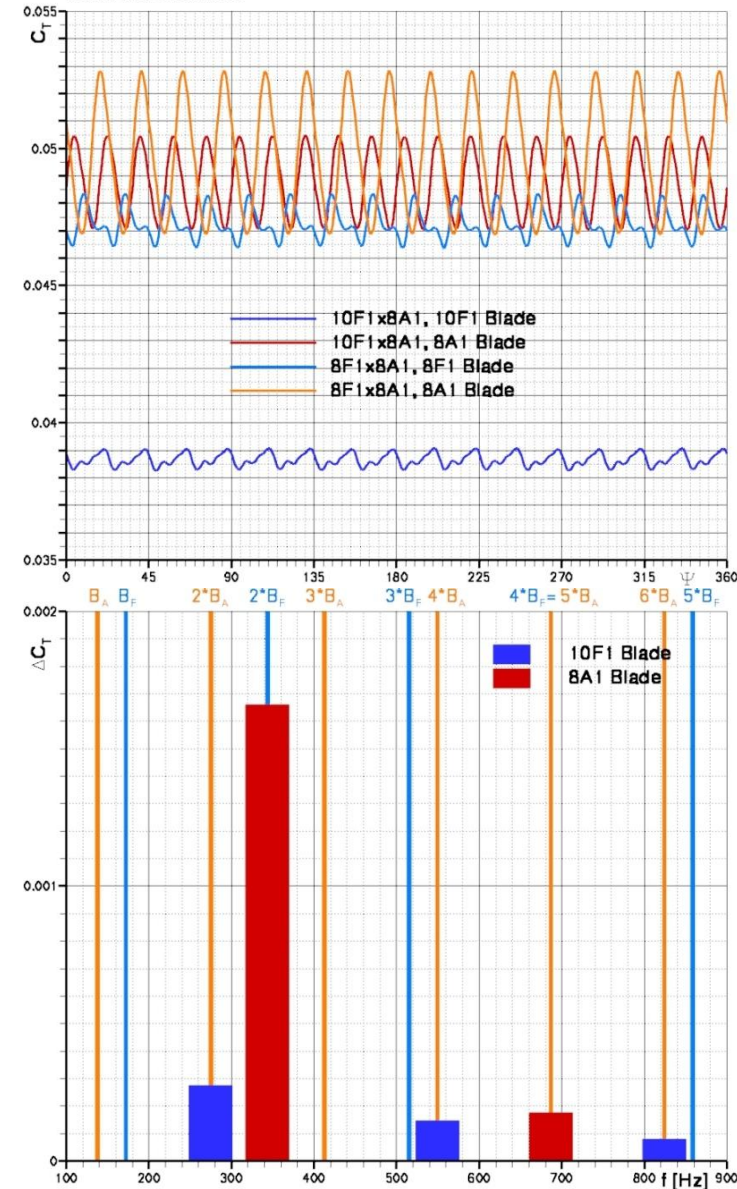
- Different blade load distributions, higher in R2 in each case
- Blades more highly loaded for 8F1x8A1
- Blades show force oscillations linked to rotor-rotor blade passage
- Front blade wakes lead to full spanwise fluctuations on aft blades (pronounced at hub and tip)
- Rotor 1 blade shows smaller oscillations
- Tip vortex impact on aft blades is dominant



Blade Force Development Low-Speed Conditions

- Higher blade thrust loadings in both rotors for the 8x8 configuration
- Higher aft blade loadings in each case
- Fluctuation amplitudes for aft blades more pronounced
- 8x8 fluctuation amplitudes greater
- Aft blades shows 16/20-cycle fluctuations (i.e. $2*B_F$)
- Front blades shows 16/32 cycle oscillations (i.e. $2*B_A$ and $4*B_A$)
- FFT Analysis of blade thrust loading:
 - Dominant $2*B_F$ fluctuations for aft blades
 - Importance of higher harmonic thrust oscillations of front blades

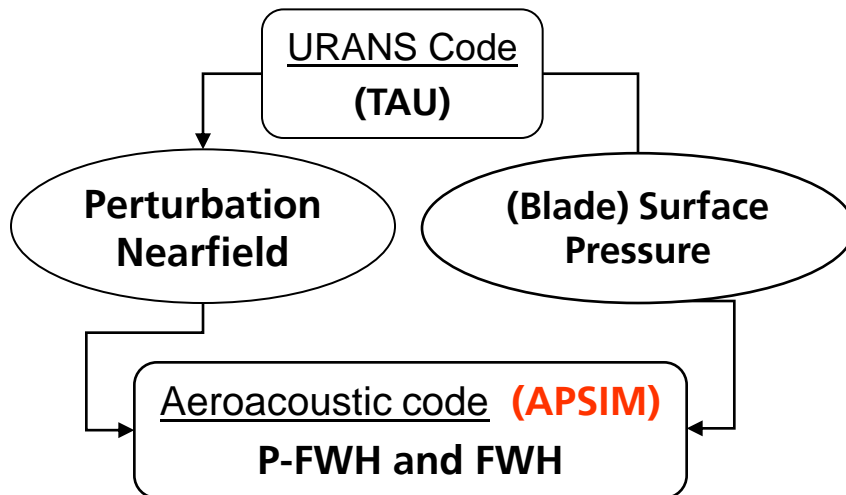
10F1x8A1 vs 8F1x8A1 TO @ SL, M=0.2, $\alpha=0^\circ$
Blade Force Coefficients



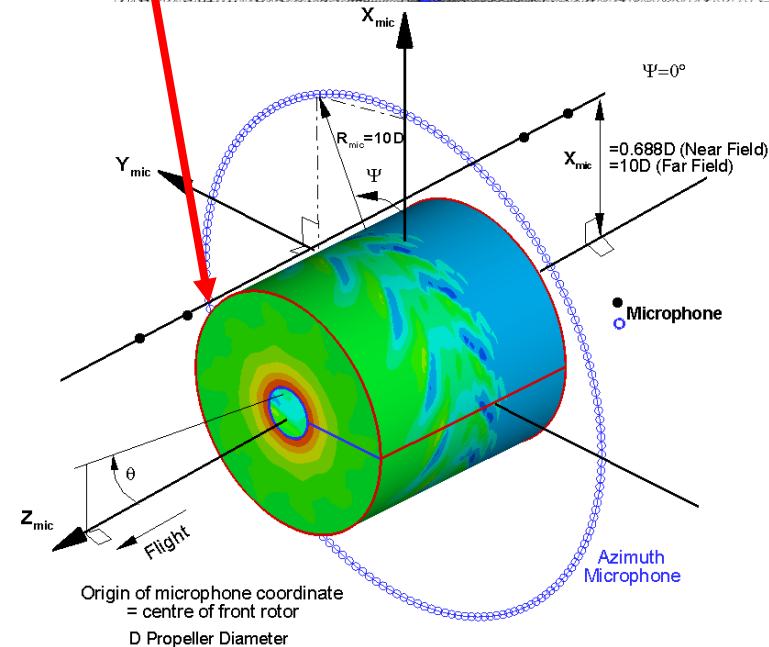
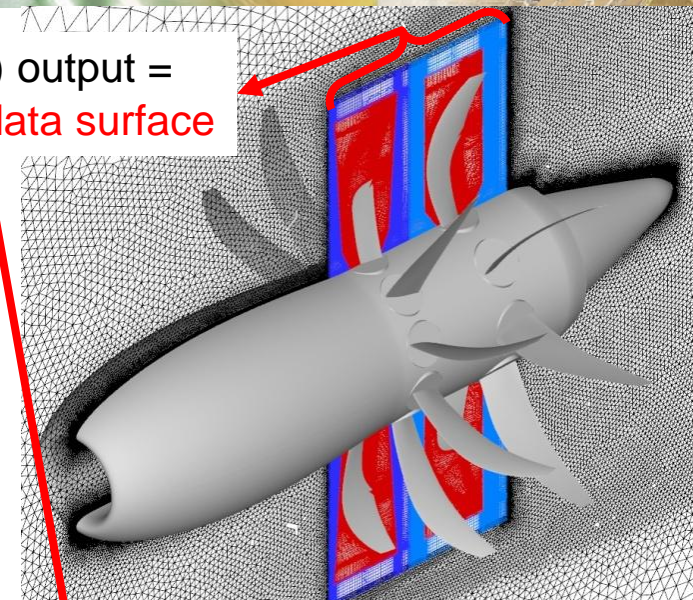
Aeroacoustic Analysis: Tools & Approach

CFD (TAU) output = FW-H input data surface

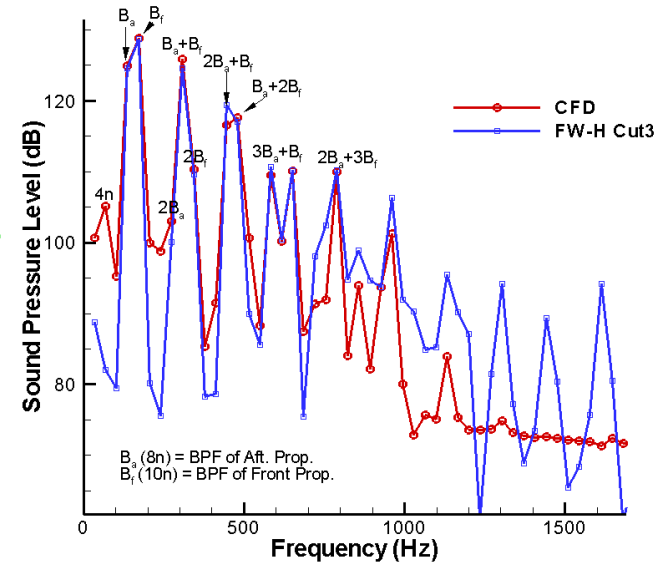
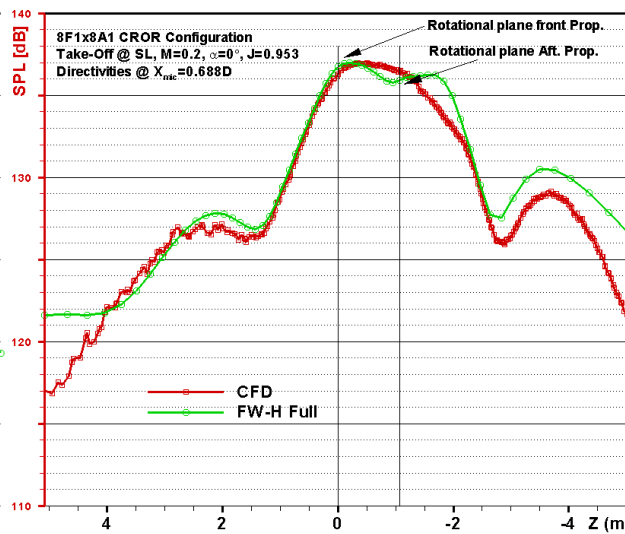
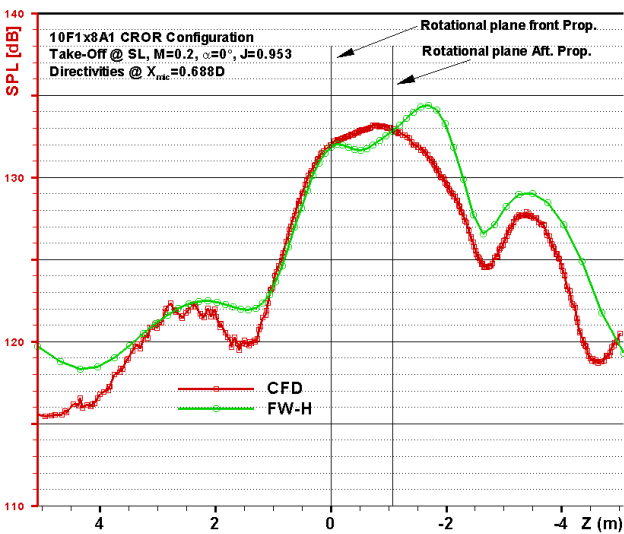
- Noise radiation analysis using APSIM (Acoustic Prediction System based on Integral Method)
 - Rotor & Propeller Noise
 - Permeable or Impermeable FW-H



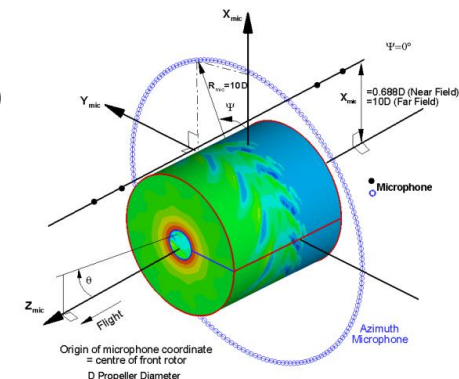
- Virtual microphones oriented around front prop center
- Nearfield mic array @ $x/D=0.688$ (~ pylon length)
- Farfield virtual mic array @ $x/D=10$
- Farfield azimuthal mic array @ $r/D=10$



Aeroacoustic Analysis: Permeable FW-H Approach Nearfield Noise Radiation @ LS



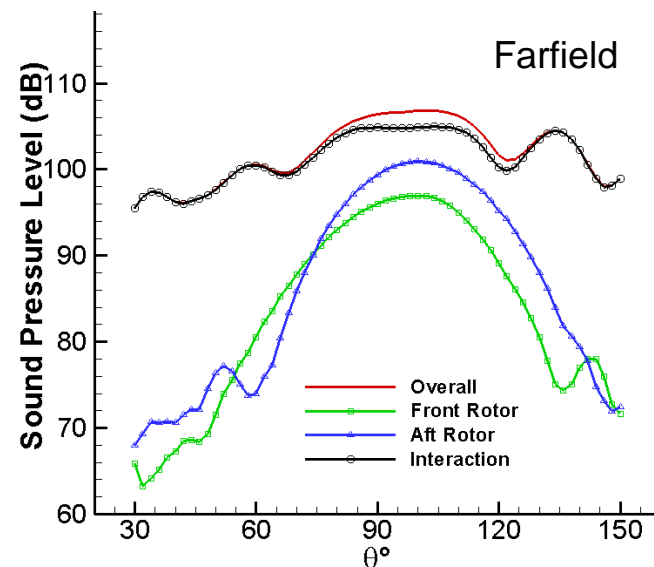
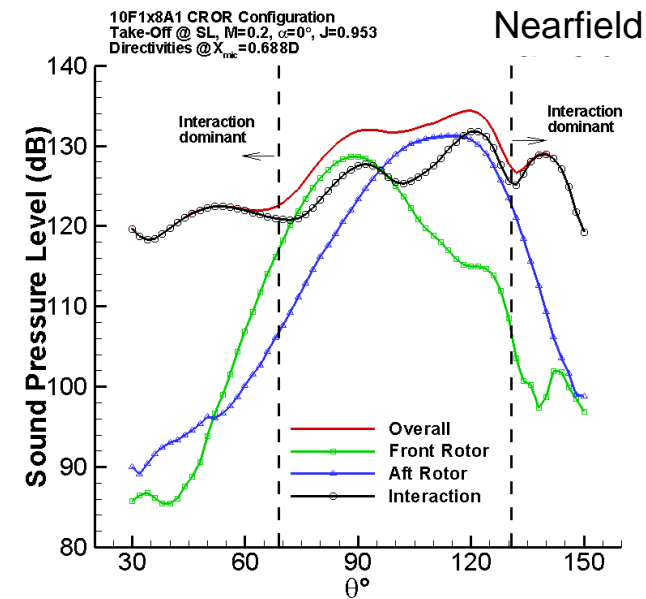
- Characteristic noise radiation signature known from literature
 - Max. noise due to rotor-alone tones near rotor planes (mono- & dipole)
 - Slightly higher noise near aft rotor due to higher loading & interactions
 - ~5dB peak noise difference between 10x8 and 8x8 configuration
- Front rotor plane spectrum:
 - Good match between FW-H and CFD for $f < 800\text{Hz}$
 - Strong rotor fundamental tones and 1st & 2nd order interaction tones



Aeroacoustic Analysis @ LS

Near- & Farfield Noise Radiation

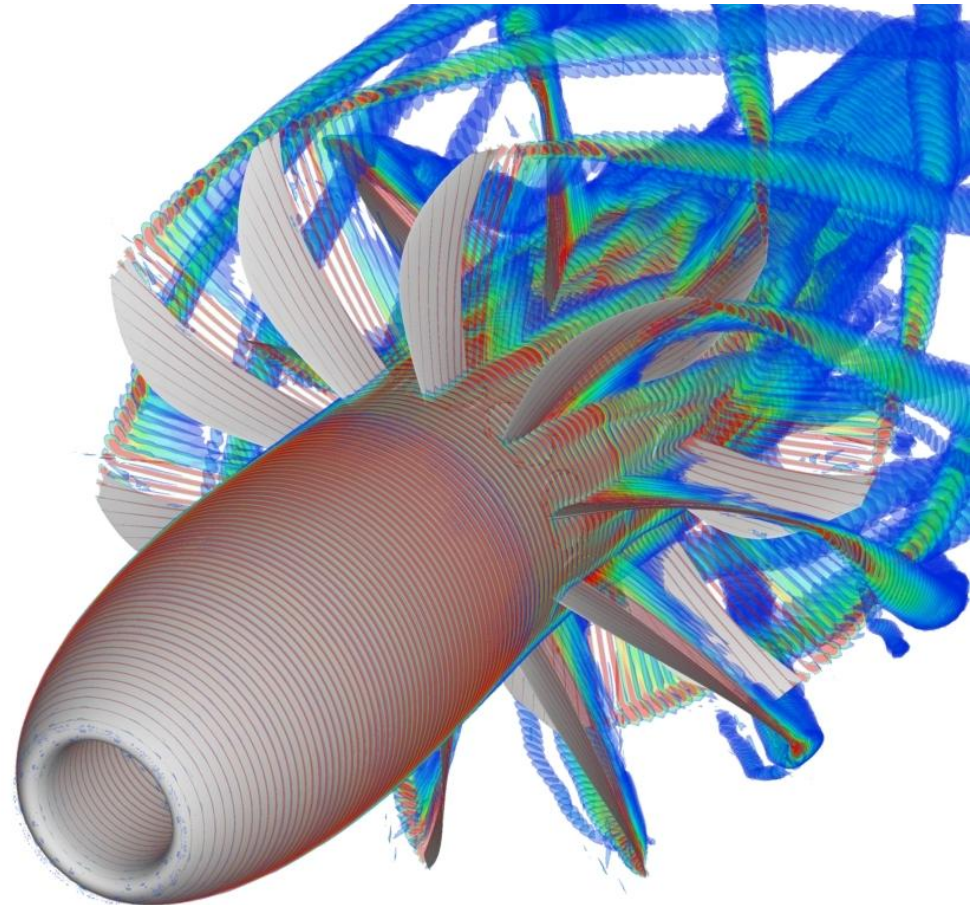
- Highest noise levels for both configurations in vicinity of rotor planes, with peaks closest to aft rotor
- Noise levels higher for 8x8 at most microphone locations
- 10x8 near-field directivity decomposition:
 - Rotor tones dominate in vicinity of planes of rotation
 - Interaction tones very important for polar angles towards the rotational axis
- 10x8 far-field directivity decomposition:
 - Interaction tones are major noise source
 - Rotor tone levels in farfield reduced more notably than interactions tones



Numerical Analysis of CROR Propulsion System Aerodynamics & Aeroacoustics at DLR

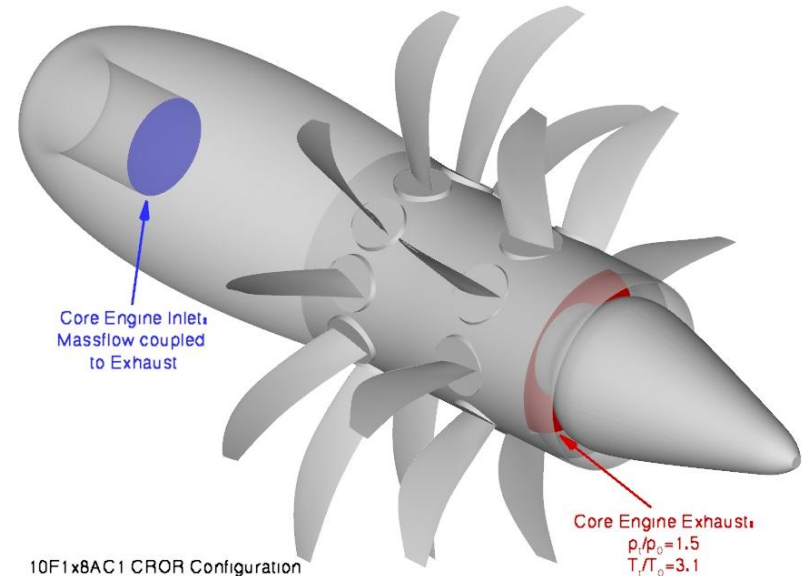
Arne Stuermer &
Jianping Yin
Institute of Aerodynamics &
Flow Technology
DLR Braunschweig
Germany

2nd UTIAS-MITACS
International Workshop on
Aviation & Climate Change
May 27th-28th, 2010
UTIAS
Toronto, Canada



Test Case Definition: Cruise

- Cruise @ $h=35,000\text{ft}$, $M=0.75$ & $\alpha=0^\circ$
- Identical propeller rotational speeds
- TAU engine boundary condition to simulate realistic inlet and jet flows
- Blade settings for an equal blade power absorption for the 10F1x8A2 configuration (i.e. power split of 1.25:1/56:44), identical disc power loading for the 10F2x8AC1 (1.45:1/x59:41)
- 10F2x8AC1 CROR:
 - $F_x=18.990\text{ kN}$
 - $C_{P,1}/C_{P,2}=1.4471$
- 10F1x8A2 CROR:
 - $F_x=19.103\text{ kN}$
 - $C_{P,1}/C_{P,2}=1.2488$



10F1x8AC1 CROR Configuration
TAU Simulation Engine Settings
Cruise @ $h=35,000\text{ft}$, $M=0.75$, $n=850\text{rpm}$

| | Core engine | | $n_1=n_2$ [rpm] | J_1 | J_2 | $\beta_{75,R1}$ [°] | $\beta_{75,R2}$ [°] |
|-----------|-------------|-----------|--------------------|-------|-------|------------------------|------------------------|
| | p_t/p_0 | T_t/T_0 | | | | | |
| 10F1x8A2 | 1.5 | 3.1 | 850 | 3.678 | 3.678 | 61.95 | 58 |
| 10F2x8AC1 | 1.5 | 3.1 | 850 | 3.678 | 4.327 | 61.95 | 63.05 |

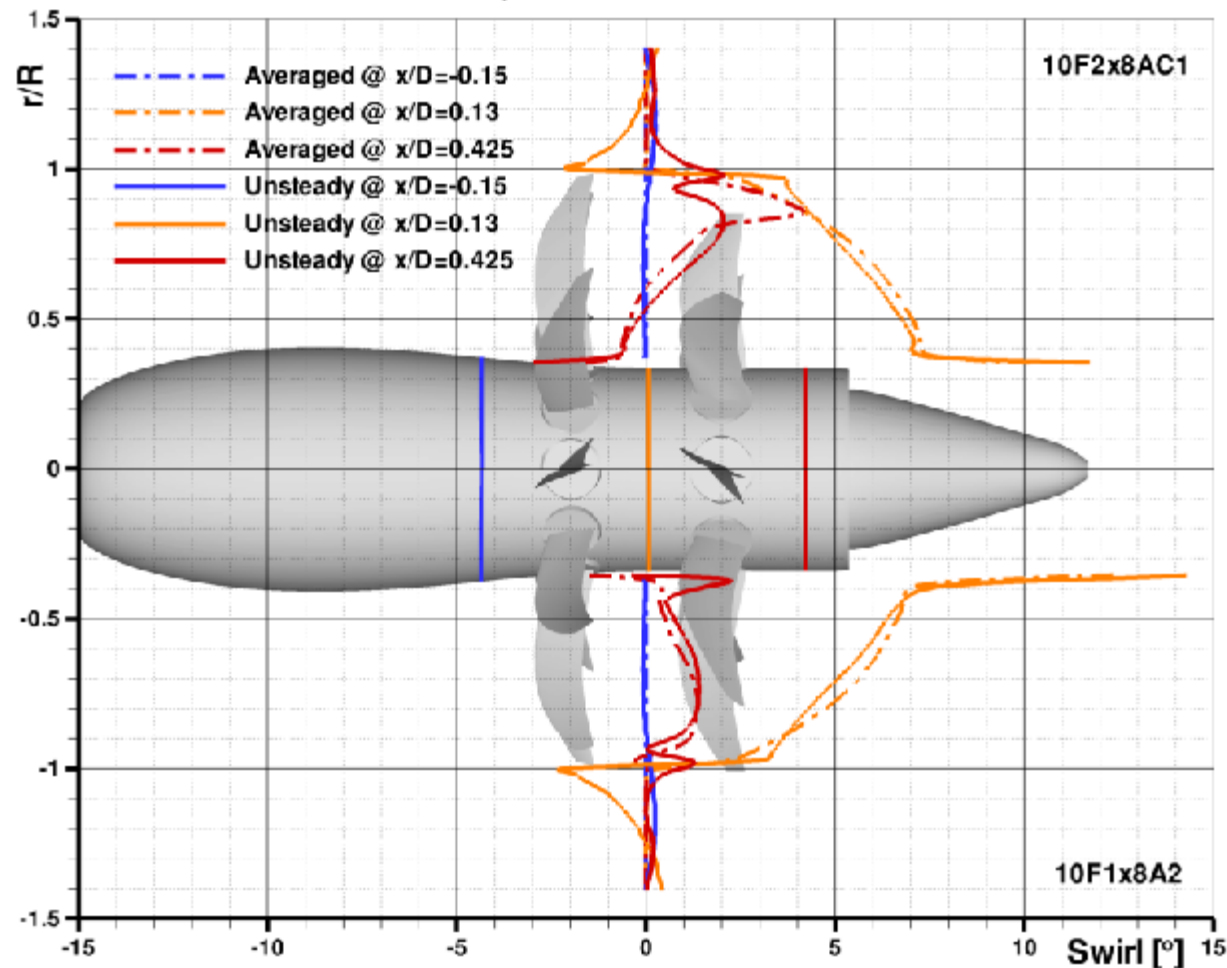
| | 10F1x8A2 | | | 10F2x8AC1 | | |
|------------|----------|---------|--------|-----------|---------|--------|
| | Rotor 1 | Rotor 2 | Total | Rotor 1 | Rotor 2 | Total |
| F_x [N] | 9,972 | 9,131 | 19,103 | 10,566 | 8,424 | 18,990 |
| C_T | 0.3934 | 0.3603 | - | 0.4169 | 0.6368 | - |
| C_P | 1.8381 | 1.4719 | - | 1.9235 | 1.1031 | - |
| η [%] | 78.73 | 90.03 | 84,38 | 79.72 | 91.98 | 85.85 |

Slipstream Development: Swirl Recovery

10F2x8AC1 vs 10F1x8A2 CROR Configuration
Cruise @ $h=35,000\text{ft}$, $M=0.75$, $\alpha=0^\circ$
Slipstream Swirl Profiles

➤ Comparison of swirl for 10F2x8AC1 & 10F1x8A2 CROR:

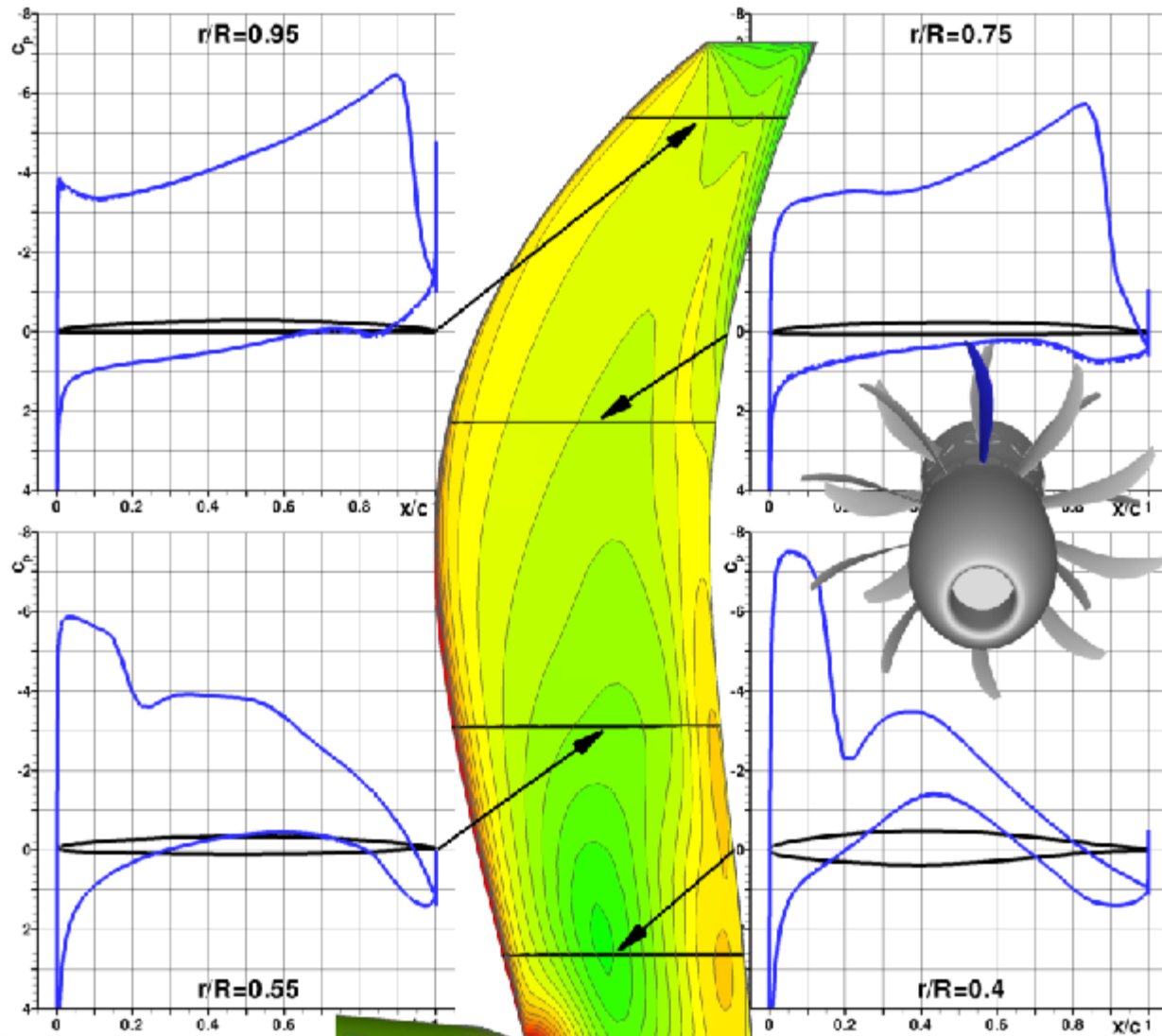
- Good swirl recovery for both configurations
- Similar front rotor loadings result in similar slipstream swirl distribution
- Cropped aft blade “misses” tip swirl recovery



Blade Pressure Distributions

10F2x8AC1

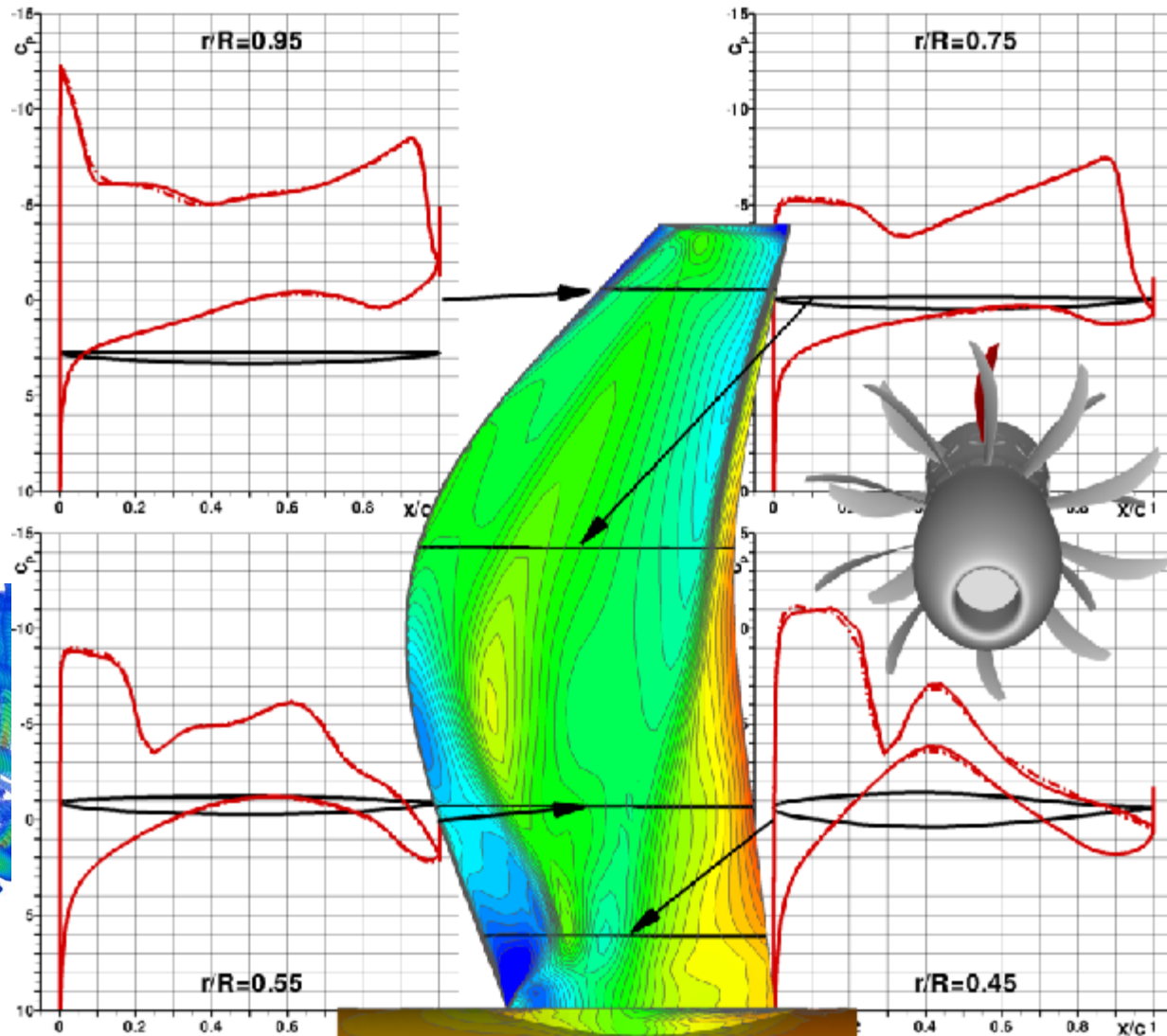
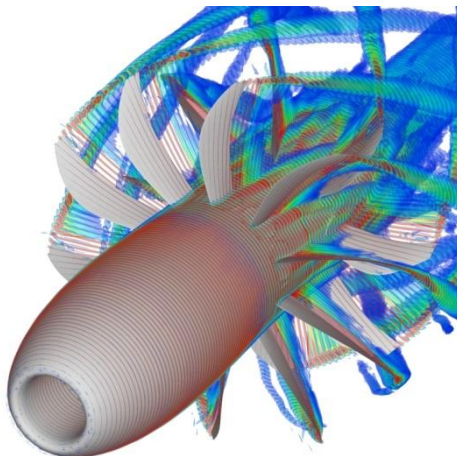
- Front blade is affected by aft blade potential flow field
- Notable pressure fluctuation visible on pressure side, in particular near the tip
- Full span transonic flow on blade suction side
 - Shock @ $x/c \sim 0.2$ near the root
 - Shock near TE towards the tip
 - No notable impact of unsteady blade-blade interactions on front rotor transonic flow (shock strength & location constant)



Blade Pressure Distributions

10F2x8AC1

- Aft blade is strongly affected by front rotor blade wakes
- Pressure and suction side show 20-cycle oscillations
- Apparent residual influence of front rotor tip vortex passage over blade tip
- Strong hub fluctuations due to PCM/blade root vortex



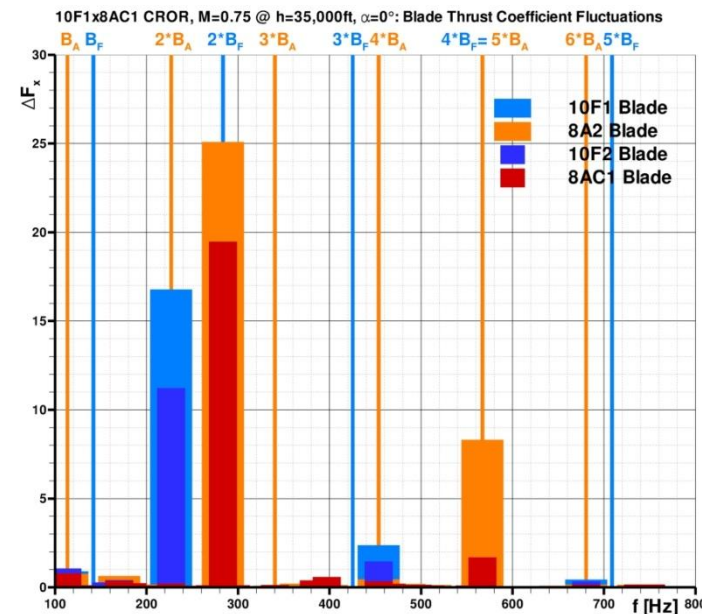
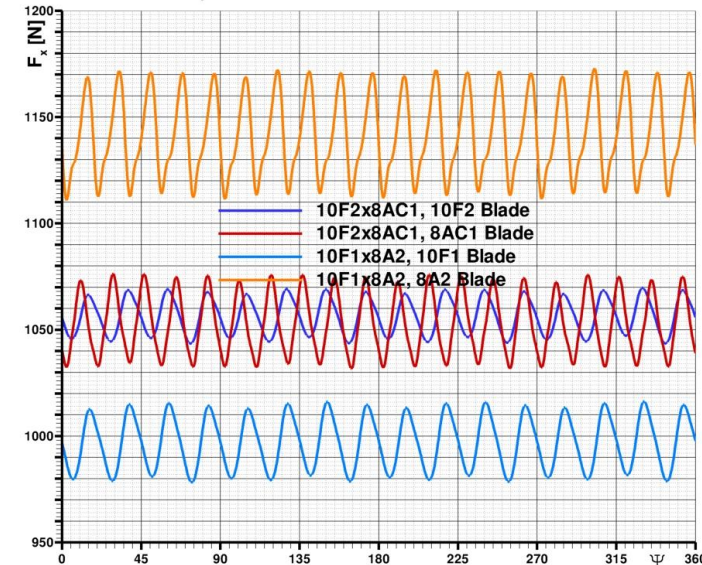
Blade Force Development Cruise Conditions

- Fluctuation amplitudes for aft blades more pronounced in each case
 - Larger amplitudes for 10F1x8A2 CROR due to tip vortex impingement

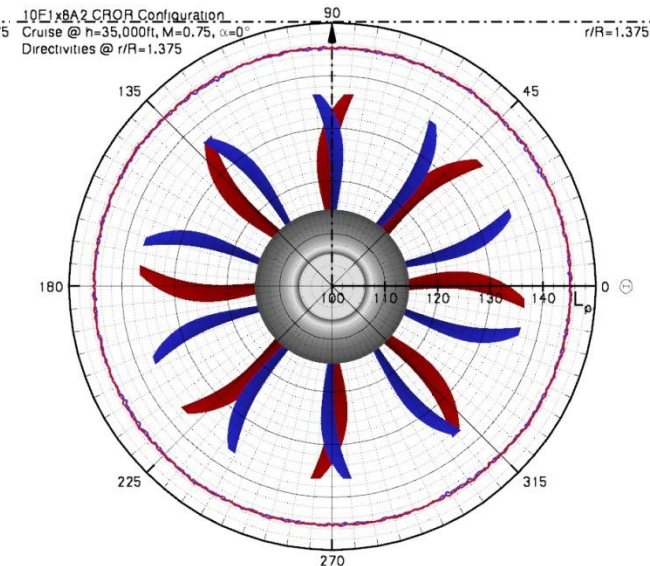
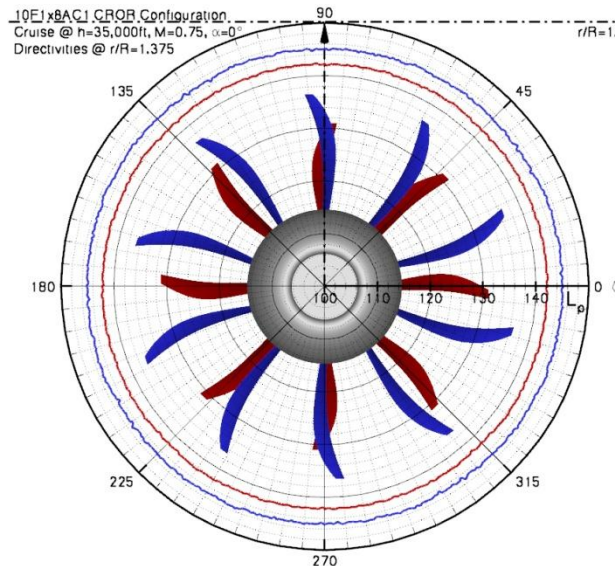
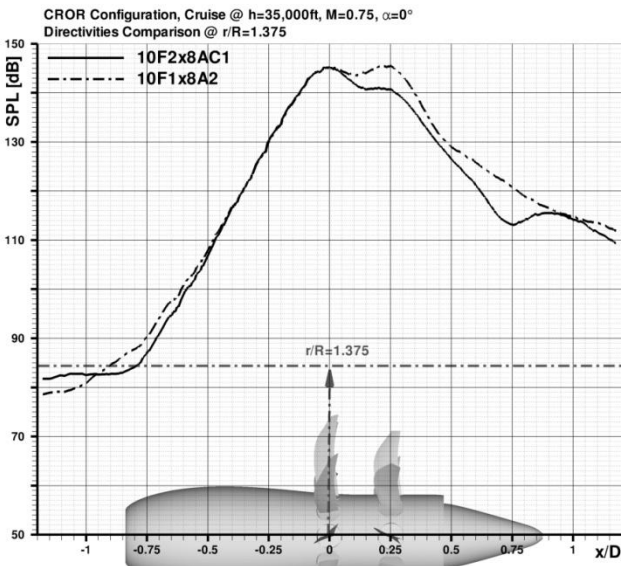
- Aft blades show 20-cycle fluctuations, i.e. @ $2 \cdot B_F$
 - Larger amplitudes for 10F1x8A2 CROR due to tip vortex impingement

- Front blades show 16-cycle oscillations, i.e. @ $2 \cdot B_A$
 - Slightly larger amplitudes for 10F1x8A2 CROR due to full-span potential flow impact of aft rotor blades

10F2x8AC1 vs 10F1x8A2 Cruise @ h=35,000ft, M=0.75, $\alpha=0^\circ$
Blade Force Development

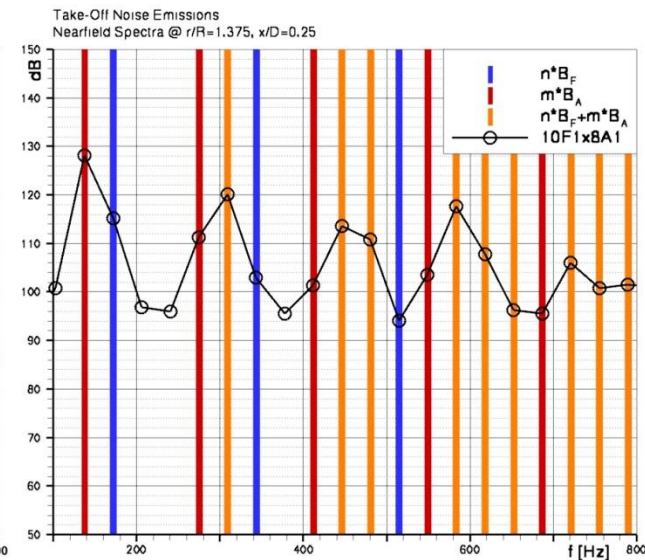
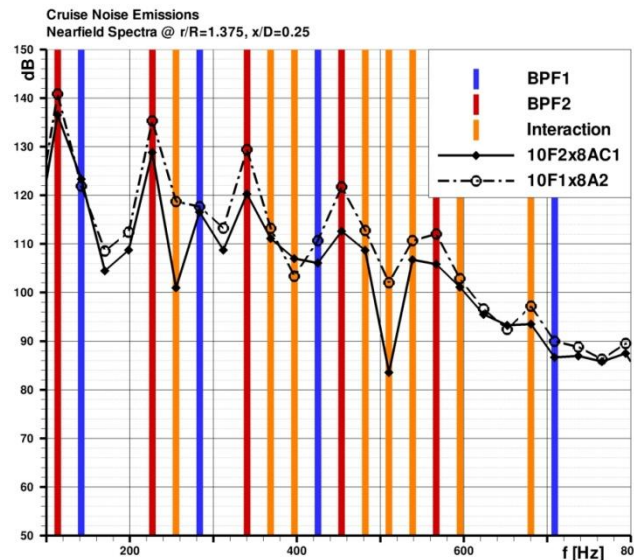
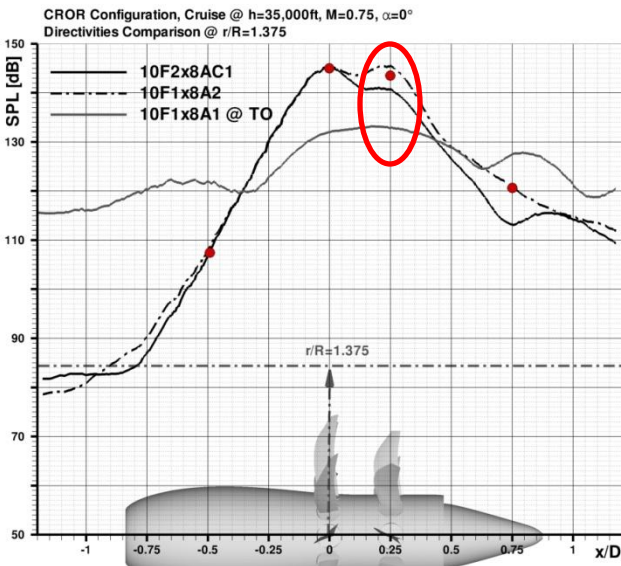


Aeroacoustic Analysis: Nearfield Directivities



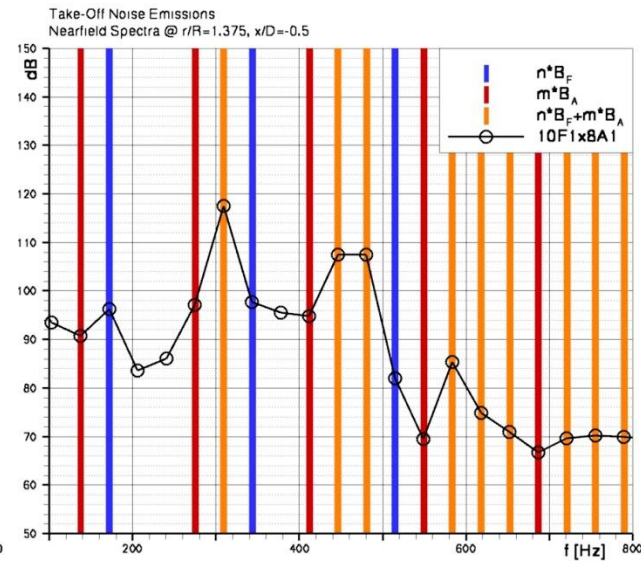
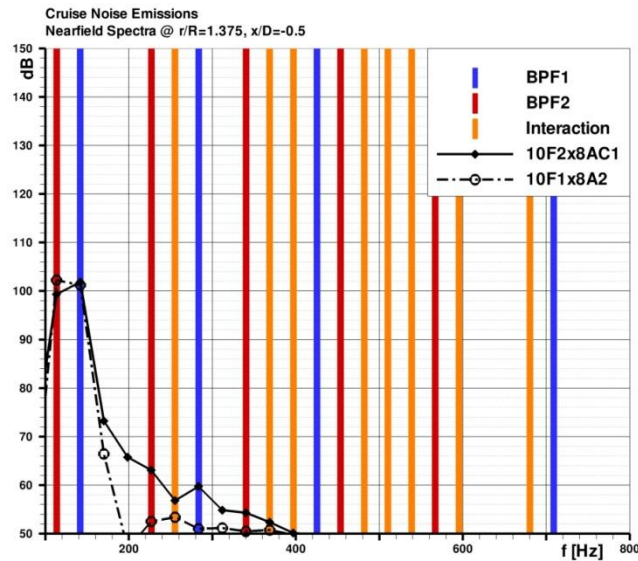
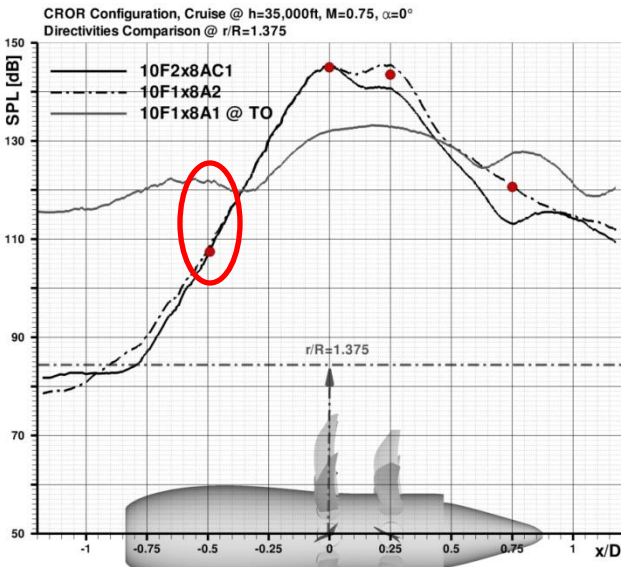
- Front rotor plane shows similar OASPLs for both configurations
 - Mean loadings near-identical → Mono- and di-pole noise similar
 - Only small differences in unsteady loadings → Unsteady loading noise similar
- Slightly higher OASPLs for 10F1x8A2 CROR in aft rotor plane
 - Unsteady loading noise dominates steady loading noise

Aeroacoustic Analysis: Nearfield Noise Spectra @ $x/D=0.25$



- Aft rotor plane noise emissions dominated by B_A and its higher harmonics
 - Slightly higher SPL @ n^*B_A for 10F1x8A2
- At low-speed conditions spectrum in the aft rotor plane also shows importance of interaction tones

Aeroacoustic Analysis: Nearfield Noise Spectra @ $x/D=-0.5$

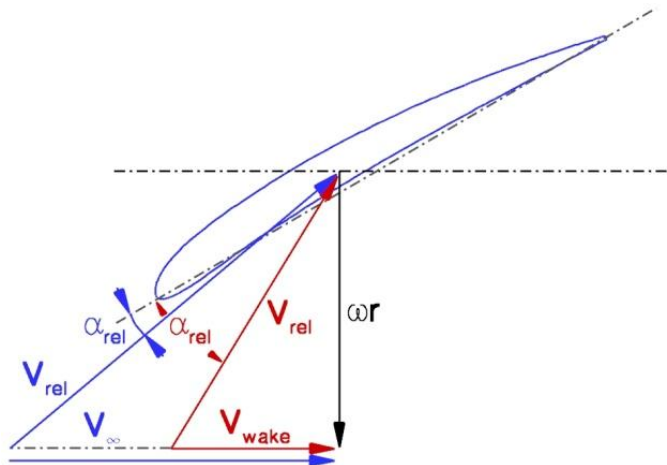


- Forward noise radiation at cruise limited to rotor BPF contributions
 - Slightly higher SPL @ B_A for 10F1x8A2
- Much richer spectrum and higher levels throughout at low-speed conditions
 - Interaction tones dominate

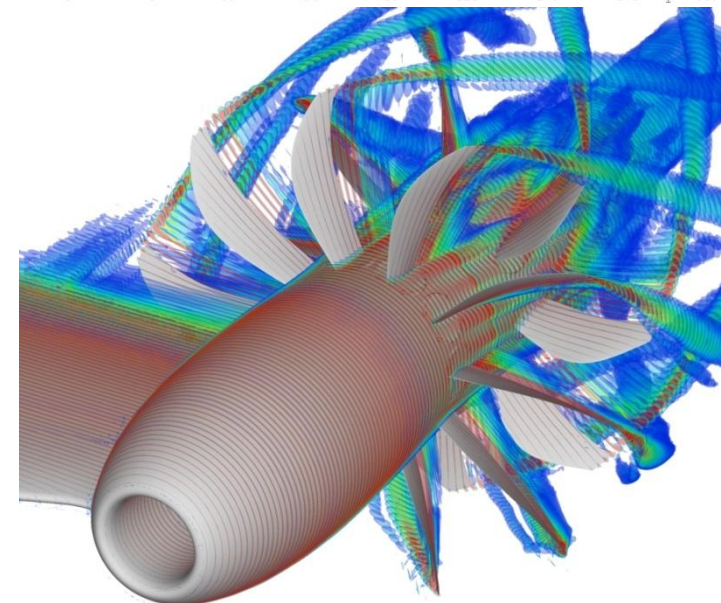
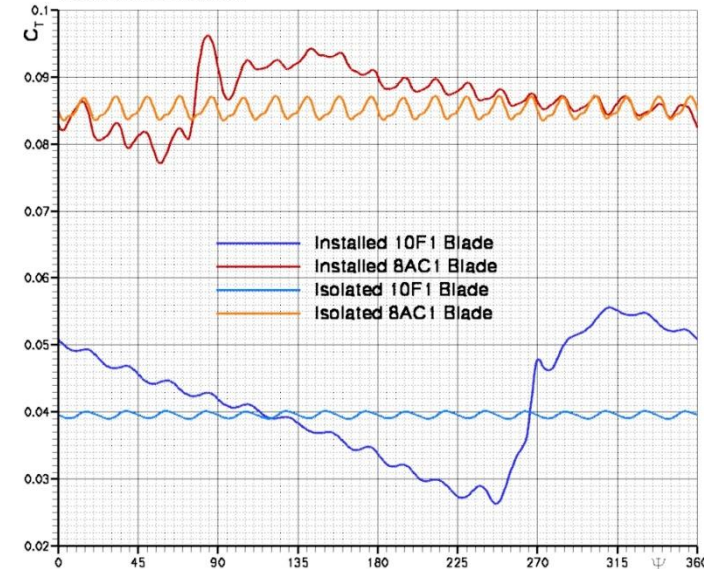


Installation Impact @ Cruise: Blade Forces

- Installation impact for identical blade settings as the isolated case leads to increased mean loadings
- Azimuthal variations of blade loadings due to local interaction with pylon wake
 - Wake increases the effective blade angle of attack



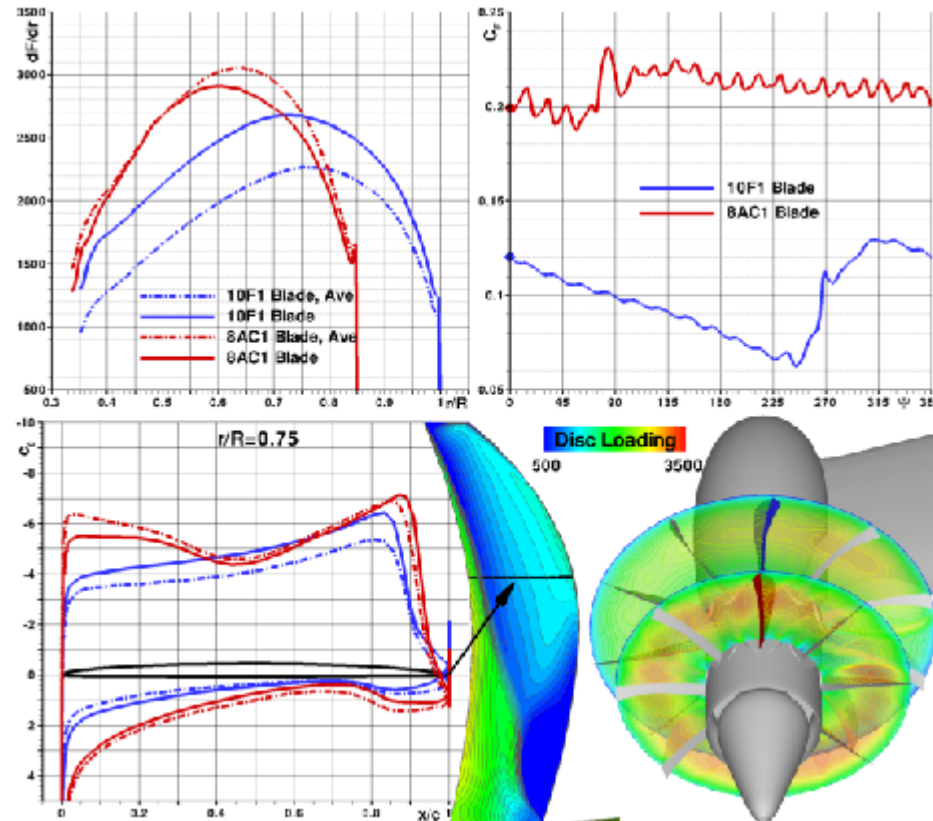
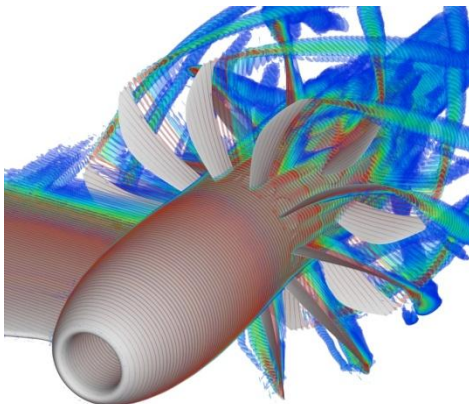
Pylon+10F1x8AC1 Cruise @ h=35,000ft, M=0.75, $\alpha=0^\circ$, $\beta_{75,R1}=62^\circ$, $\beta_{75,R2}=63.75^\circ$
Blade Force Development



Installation Impact on Blade Pressure Distributions

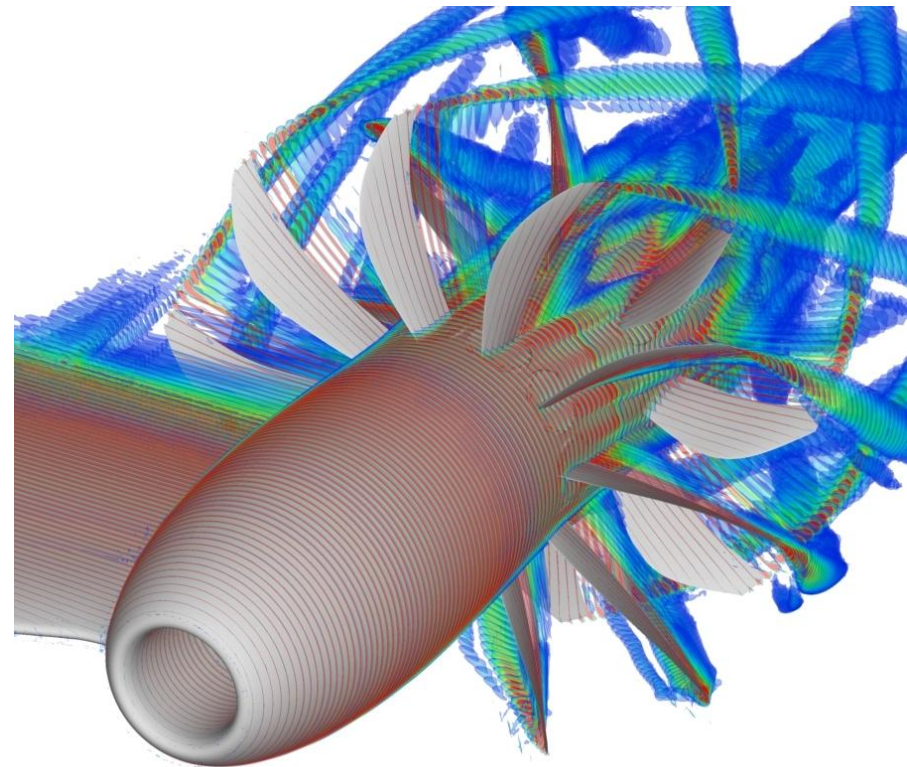
10F1x8AC1

- Front blade affected by aft blade potential flow
- Notable pressure fluctuation visible on pressure side, in particular near the tip
- Full span transonic flow on blade suction side
- Pylon wake leads to local increase in blade angle of attack
 - Strong impact on suction side transonic flow
 - Global effects are azimuthal blade loading variations



Conclusions & Outlook

- Established process chain for coupled Hi-Fi TAU uRANS & aeroacoustic simulations with the DLR APSIM code allows for an in-depth analysis, enhancing understanding of complex interactions
- Better understanding of requirements for good quality data
- Outlook on planned future activities:
 - CROR configuration/operating point studies, 1P-Loads & installation effects
 - Passive and active noise control technologies: Pylon and front rotor blade trailing edge blowing; front rotor blade trailing edge serrations (DLR-AT)
- Perspective:
 - Maybe Hi-Fi CFD and CAA can contribute to making Open Rotor work this time around



Numerical Analysis of CROR Propulsion System Aerodynamics & Aeroacoustics at DLR

Arne Stuermer &
Jianping Yin
Institute of Aerodynamics &
Flow Technology
DLR Braunschweig
Germany

2nd UTIAS-MITACS
International Workshop on
Aviation & Climate Change
May 27th-28th, 2010
UTIAS
Toronto, Canada

